Published in final edited form as:
Biochemistry. 2011 May 31; 50(21): 4615–4622. doi:10.1021/bi200321c.

Streptomyces clavuligerus HlmI is an intramolecular disulfide-forming dithiol oxidase in holomycin biosynthesis

Bo Li and **Christopher T. Walsh***
Department of Biological Chemistry & Molecular Pharmacology, Harvard Medical School, 240 Longwood Ave, Boston, MA 02115, USA

Abstract

Holomycin and related dithiolopyrrolone antibiotics display broad-spectrum antimicrobial activities and contain a unique 5, 5-bicyclic ring structure with an N-acylated aminopyrrolone fused to a cyclic ene-disulfide. Here we show that the intramolecular disulfide bridge is constructed from the acyclic ene-dithiol at a late stage in the pathway by a thioredoxin oxidoreductase-like enzyme HlmI from the holomycin producer *Streptomyces clavuligerus*. Recombinant HlmI was purified from *E. coli* with bound flavin adenine dinucleotide (FAD), and converts reduced holomycin to holomycin utilizing O_2 as cosubstrate. As a dithiol oxidase, HlmI is functionally homologous to GliT and DepH, which perform a similar dithiol to disulfide oxidation in the biosynthesis of fungal natural product gliotoxin and epigenetic regulator compound FK228 respectively. Deletion of the *hlmI* gene in the wild type *S. clavuligerus* and in a holomycin-overproducing mutant resulted in decreased level of holomycin production and increased sensitivity toward holomycin, suggesting a self-protection role of HlmI in the holomycin biosynthetic pathway. HlmI belongs to a new clade of uncharacterized thioredoxin oxidoreductase-like enzymes, distinctive from the GliT-like enzymes and the DepH-like enzymes, and represents a third example of oxidoreductases that catalyzes disulfide formation in the biosynthesis of small molecules.

Natural product antibiotics holomycin and its variants, such as thiolutin, aureothricin, xenorhabdin and thiomarinol, share a common N-acylated bicyclic dithiolopyrrolone scaffold (also known as pyrrothine) (Figure 1A) (1–4). These dithiolopyrrolone antibiotics have been reported to interfere with bacterial RNA synthesis (5–7), however, the mode of action and the relevance of the disulfide to activity remains unclear as direct inhibition of RNA polymerases has yet to be reconstituted *in vitro* (7).

Disulfides are present in a wide variety of natural products, in larger ribosomally-encoded constructs, e.g. conotoxins and cyclotides, as well as smaller, non-ribosomal peptides such as gliotoxin and the antitumorigen FK228. In all of these natural products, the disulfide is essential for the activity of the molecule. In the cyclotides, cystine disulfides impart increased thermal stability, conformational rigidity, and cell permeability (8). Similarly, in FK228, the disulfide has been shown to promote cell permeability while masking the active form containing free thiol of the epigenetically active prodrug (9). The mycotoxin, glyotoxin employs the disulfide in two complimentary and damaging activities: 1) redox cycling to produce destructive superoxide free radicals and 2) crosslinking and inhibition of cellular proteins *via* formation of mixed disulfides with the reduced form (10). Given the importance

*To whom correspondence should be addressed: christopher_walsh@hms.harvard.edu, Phone: 617.432.1715, Fax: (+1) 617.432.0483.

Supporting Information available
Supporting information includes Figures S1–8 and Table S1. This material is available free of charge via the Internet at http://pubs.acs.org.

of the disulfide linkage to stability and mobility of these molecules, it is of considerable interest as to when and how the disulfides are installed in the mature natural products. Formation of disulfides in FK228 and gliotoxin is catalyzed by thioredoxin reductase-like enzymes DepH and GliT, both of which are encoded in their respective biosynthetic gene clusters (Figure 1B) (11, 12). Prior to the work reported herein, it was unclear which enzyme may be responsible for generation of the unusual disulfide present in holomycin.

We recently identified the holomycin biosynthetic gene cluster through genome mining of the producing bacterium *S. clavuligerus* (13). In addition to a nonribosomal peptide synthetase (NRPS) module which activates and loads the essential building block L-Cys and an acetyl transferase for introduction of the N-acetyl moiety, four predicted flavin-dependent oxidoreductases are encoded in the gene cluster (Figure 2A). The presence of four such oxidoreductases is consistent with a pathway where L-Cys-L-Cys undergoes oxidations removing a net total of eight electrons in four two-electron oxidation steps, each catalyzed by one of the flavoenzymes (Figure 2B). One of the flavoenzymes, HlmI, displays homologies to the large family of thioredoxin reductases, involved in dithiol-disulfide redox interconversions in protein substrates. We demonstrate that HlmI is a dithiol oxidase, converting the reduced dithiol form of holomycin (*red*holomycin), **2**, to the disulfide form, **1**, (Figure 1B). Heterologous expression of the holomycin gene cluster in *S. albus* was recently reported by Deng H. and coworkers and deletion of the *hlmI* gene abolished holomycin production, suggesting a role for HlmI in holomycin biosynthesis (14).

Material and Methods

Molecular cloning of *hlmI*, and overexpression and purification of the HlmI protein

The *hlmI* gene was cloned into pET30-Ek/LIC vector (Novagen) using primers listed in Table S1 and the gene sequence was verified by DNA sequencing. This vector was introduced into BL21-CodonPlus (DE3)-RIPL chemical competent cells (Stratagene). A 2 L LB broth with 20 mL of overnight culture was started from single colonies and protein overexpression was induced at an OD_{600nm} of 0.6 with 0.2 mM isopropyl-β-D-thiogalactopyranoside (IPTG) at 18 °C for 18 h. The cells were harvested by centrifugation, resuspended in 20 mL of column buffer (50 mM HEPES, 300 mM NaCl, 10% glycerol, pH 7.5) and lysed with a cell disruptor. The lysis mixture was clarified by ultracentrifugation and the supernatant was incubated with 2 mL of Nickel-NTA agarose resin (Qiagen) at 4 °C with gentle mixing for 1 h. The resin with bound protein was loaded on to a column to drain the flowthrough, washed with 50 mL of column buffer and 20 mL of column buffer containing 20 mM imidazole, and eluted with 10 mL of elution buffer (300 mM imidazole in column buffer). The elution fractions were analyzed by SDS-PAGE and the fractions containing HlmI were pooled and concentrated to 5 mL with a 15-mL Amicon (Millipore) (10kDa MW cutoff). Concentrated protein was desalted with a PD-10 desalting column (GE Healthcare) twice to remove excess imidazole. The resulting protein was flash frozen with liquid N_2, and stored at −80 °C.

Molecular cloning of *gliT*, overexpression, and purification of the GliT protein

Aspergillus fumigatus Af293 cDNA was a gift from Robert A. Cramer Jr. (Durham, NC) (15). Using this cDNA as template, *gliT* was amplified by PCR and cloned into pET24b between NdeI and XhoI sites. The sequence was verified by DNA sequencing. BL21 (DE3) cells containing the constructed vector were grown overnight at 37 °C. A 6 Liter of LB containing 40 μg/mL kanamycin and 5 mM $MgCl_2$ was inoculated with 1% of the overnight culture. When OD_{600nm} of the culture reached 0.7, protein expression was induced with 0.1 mM IPTG and the culture was grown for additional 12 hours at 15 °C. Cells were harvested and resuspended in 28 mL lysis buffer (25 mM Tris, pH 8.0, 500 mM NaCl), lysed with two

passes on an Emulsiflex-C5 cell disruptor (Avestin). Cell lysate was cleared at 35000 ×rpm (95000 ×g) for 35 min, and incubated with 1.1 mL Ni-NTA resin (2.2 mL 50% slurry) that was prewashed with lysis buffer for 1.5 hours at 4 °C. Resin was then transferred to column and a gradient imidazole elution was performed: 25 mL for 0 and 5 mM imidazole, 15 mL for 25 mM, 10 mL for 200 mM and 5 mL for 500 mM imidazole. GliT was eluted in the 25, 200 and 500 mM imidazole elution fractions, which were combined and concentrated to less than 2 mL and injected for gel filtration in 20 mM Tris, pH 8, 50 mM NaCl. Fractions containing GliT were pooled and concentrated and 10% glycerol was added. A total of 4.5 mL of GliT was obtained, and its concentration was determined by Bradford as 294 μM.

Determination of HlmI oligomeric state and FAD content in HlmI and GliT

Purified HlmI was analyzed by size exclusion chromatography using a 10/300 Superdex 200 gel-filtration column and running buffer containing 50 mM HEPES, 150 mM NaCl, and 5% glycerol at pH 7.5. The calculated molecular weight for HlmI is 39163 Da, and the apparent molecular weight for HlmI is approximately 80 kDa based on the standard curve on the gel filtration column suggesting that HlmI exists as a dimer. Both HlmI and GliT were denatured by boiling for 5 min to release the flavin cofactor. The supernatant was injected on Accurate-Mass Q-Tof LC/MS instrument (Agilent Technologies 6520) and the flavin cofactor was identified as FAD. To measure the FAD content, UV scan between 200 nm and 600 nm (Cary UV-vis) were taken for HlmI and GliT and also the FAD-containing supernatant from the denatured samples. Absorbance at 450 nm for the latter samples was used to determine the concentration of FAD using extinction coefficient 11300 M^{-1} cm^{-1}, and the background absorbance at 280 nm from FAD was subtracted from the A_{280nm} values of the non-denatured HlmI and GliT samples. The adjusted A_{280nm} values were used for calculation of protein concentrations using theoretical extinction coefficients 26595 M^{-1} cm^{-1} for HlmI and 30160 M^{-1} cm^{-1} for GliT. Duplicate experiments were performed and the average FAD content was 20% for HlmI and 35% for GliT. To reconstitute the binding of FAD in HlmI and GliT, both proteins were incubated with excess FAD on ice for 30 min. Excess FAD was removed by passing the proteins through Micro Bio-Spin 6 Chromatography columns pre-equilibrated in buffer containing 20 mM Tris, 10 mM NaCl, 5% glycerol (pH 8.5). HlmI was further purified using a MonoQ 10/100 GL anion exchange column (GE Healthcare). A linear gradient from 10 mM NaCl to 1 M NaCl was run over 7 column volumes at 1 mL/min. Fractions containing HlmI were combined and concentrated using Amicon Ultra centrigual filters (0.5 mL, 3kDa molecular weight cutoff). The resulting protein was shown to be over 95% pure by SDS-PAGE. The FAD content was determined using the same method as described above and increased to 80% and 76% in GliT and HlmI respectively.

Enzymatic assays to measure steady-state kinetic parameters

Holomycin was isolated from overproducing strain *S. clavuligerus* ΔORF15 and purified by HPLC as previously described (13). The concentration of holomycin was calculated based on UV absorbance at 388 nm using a reported extinction coefficient of 11220 $M^{-1}cm^{-1}$ (16). Reduced holomycin was generated by reduction of holomycin with one molar equivalent of TCEP in the presence of 100 mM phosphate buffer (pH 6.5), and a sample of 3 μl of 2 μM HlmI (50 nM final total concentration, 10 nM effective concentration) or 3 μl of 1 μM GliT (25 nM final total concentration, 8.75 nM effective concentration) was added to initiate the reaction (total reaction volume 120 μL). Because of the detectable non-enzymatic oxidation by O_2, multiple concentrations for HlmI and GliT were tested to find oxidation rates that are well above background yet still in the linear range, and the optimal concentrations for HlmI and GliT are 50 nM and 25 nM respectively. Initial velocity was measured in a continuous assay by taking a UV scan (Cary UV-vis) from 200 nm to 600 nm every 0.2 min for a total of 10 min at reduced holomycin concentrations of 5 μM, 10 μM, 25

μM, 50 μM, and 100 μM. Initial velocity was calculated from the decrease in absorbance of reduced holomycin at 340 nm with a extinction coefficient at 15900 $M^{-1}cm^{-1}$. This extinction coefficient was obtained by fully converting a solution of holomycin of known concentration to reduced holomycin with excess TCEP and measuring the absorbance at 340 nm. Background oxidation by O_2 was taken for each substrate concentration without enzyme. The enzyme catalyzed rate was obtained by subtracting the non-enzymatic rate from the overall rate. These experiments were carried out in duplicates for calculation of error. Data were analyzed and plotted using GraphPad Prism. Kinetic measurement was also performed with the FAD-reconstituted HlmI and GliT, which contained a much higher percentage of FAD, at a concentration of 25 nM (76% FAD, 19 nM effective concentration) and 12.5 nM (80% FAD, 10 nM effective concentration) respectively.

Determination of half life of reduced holomycin and reduced holothin

Holothin was generated by microwave-assisted deacetylation of holomycin dissolved in 1, 3-dioxane and heated at 100 °C for 10 min in the presence of 2N HCl. The water layer of product mixture was vacuum-dried and resuspended in water, and further purified by HPLC. A sample of 50 μM holomycin or holothin was mixed with 1 equivalent of TCEP in the presence of 100 mM phosphate buffer (pH 6.5) to generate reduced holomycin or reduced holothin. The conversion from the reduced form to the disulfide form was monitored continuously by UV. Absorbance at 340 nm and 335 nm were used respectively to calculate the half-life of reduced holomycin and reduced holothin. Data were analyzed and plotted using GraphPad Prism.

Genetic deletion of *hlmI* gene in *S. clavuligerus*

Deletion of *hlmI* gene was achieved using ReDirect PCR-targeting strategy (17). The *hlmI* gene with a 2 kb extension of the chromosomal sequence on each end was cloned into a PCR-Blunt vector (Kan^R, Invitrogen). This vector was introduced into *E. coli* BW25113/pIJ790 strain allowing for λ red mediated recombinantion. The resulting strain was transformed with PCR fragments containing the desired antibiotic resistance cassette including a 36-nt extension homologous to the target region directly upstream and downstream of the *hlmI* gene. Correct recombined vectors containing the desired disruption cassettes were selected based on antibiotic resistance. The apramycin resistance cassette was constructed using pIJ773 ($Apra^R$, *acc(3)IV-oriT*) vector as template for disruption in *S. clavuligerus* wild type. The vector pIJ10700 (Hyg^R, *hyg-oriT*) was used as template for generating the hygromycin B resistance cassette to target the ORF15::*apr* holomycin-overproducing mutant, which already contains an apramycin resistance marker. Both pIJ vectors were obtained from John Innes Centre, Norwich, UK. The *E. coli* WM6062 strain containing the disruption vectors was conjugated with the wild type or ORF15::*apr S. clavuligerus* strains following stardard protocols (18). Correct exoconjugants resulting from homologous recombination were selected based on antibiotic resistance and verified by PCR using an internal primer for the disruption cassette (pIJ773-RP603: 5'- GAG TTG TCT CTG ACA CAT TCT GGC G -3', or pIJ10700-FP1000: 5'-GGG AAC ACC GTG CTC ACC -3') and an external primer that anneals to *hlmF* gene (Scl-HlmF-LICFP: 5'-GGT ATT GAG GGT CGC ATG GAA AAT CCG ATC CCC TCT CCT TC -3'). The PCR products were also purified and verified by DNA sequencing.

Analysis of holomycin production by *hlmI* deletion mutants

The correct Δ*hlmI* deletion mutants were grown in TSB media for 24–48hr. A sample of 10 mL of liquid GSPG (glycerol-sucrose-proline-glutamate) medium (19) was inoculated with 10 μL of the starter culture and grown with shaking at 30 °C for 3–5 days. The resulting culture supernatant was filtered with Spin-X centrifuge tube filters (Corning) and a sample of 10 μL was injected on the Accurate-Mass Q-Tof LC/MS instrument (Agilent

Technologies 6520) for detection of holomycin production via Electrospray Ionization (ESI).

Agar diffusion assays to test holomycin sensitivity of *S. clavuligerus* strains

Spore stocks were prepared for wild type, Δ*hlmI*, ΔORF15, and ΔORF15/Δ*hlmI* strains. The spore concentrations were determined by serial dilutions of the stock and counting of colony forming units. Approximately 5×10^5 spores were plated for each strain and a sample of 5 μL of 7 mg/mL holomycin was added to the center of the MYM plate (4.0 g yeast extract, 10.0 g malt extract, 2.0 g dextrose, and 20.0 g agar per liter of media). The plates were incubated at 30 °C for 4–7 days and the diameter of the inhibition zone was determined as a measurement for the sensitivity of these strains toward holomycin.

Phylogenetic Analysis of HlmI

HlmI was aligned with a number of bacterial and fungal thioredoxin-oxidoreductase like enzymes from the protein data base using ClustalX. Alignment was edited using MacClade and imported into RAxML for generation of dendrogram by maximum likelihood (20). The resulting dendrogram was further colored by Adobe Illustrator.

Results and Discussion

Holomycin biosynthetic gene cluster nomenclature

Previously we demonstrated that ORFs 3483–3496 from the *S. clavuligerus* genome (locus tag SSCG_03483 through SSCG_03496) constitute a likely holomycin biosynthetic gene cluster by both genetic manipulation and biochemical characterization of ORFs 3483 and 3488 (13). In this work we renamed ORFs 3483–3496 as *hlmA*-*hlmM* (Figure 2A) where *hlm* stands for holomycin and is a three letter acronym not used elsewhere in bacterial gene assignments. ORF3492 as the focus of this work is renamed as *hlmI*.

Preparation and characterization of reduced holomycin

The disulfide formation is proposed to occur at late stages of holomycin assembly via oxidation of the dithiol groups in reduced holothin (*red*-holothin) or *red*-holomycin, **2** (Figure 2B). Because a large quantity of holomycin was readily available from a previously described overproducing strain of *S. clavuligerus* (21), we first reduced holomycin with tris(2-carboxyethyl)phosphine (TCEP) to generate *red*-holomycin, **2**, as a substrate for enzymatic analysis. LC-MS analysis of the TCEP reduction mixture showed chromatographic separation of **1** ($[M + H]^+$ expected 214.9943, observed 214.9954) from **2** ($[M + H]^+$ expected 217.0100, observed 217.0111), which was eluted earlier than holomycin on the C18 column and showed two mass unit increase in molecular weight (Figure 3A) as anticipated. The conversion of the disulfide form to the dithiol form of holomycin by TCEP resulted in a significant blue shift of the λ_{max} of UV absorbance from 385 nm in **2** to 340 nm in **1** with an approximate 50% increase in extinction coefficient to 15,900 $M^{-1}cm^{-1}$ (Figure 3B). The reduction of holomycin to *red*-holomycin is consistent with prior findings from Hertweck and colleagues that TCEP generates the reduced form of gliotoxin (11). The change in UV absorbance affords an analytical method for monitoring the reduction-oxidation reaction described below.

S. clavuligerus HlmI is an FAD-dependent oxidase for reduced holomycin

Among the four predicted flavoenzymes in the *S. clavuligerus* cluster, HlmI shares sequence homology with thioredoxin oxidoreductase superfamily (Figure S1), in particular the recently characterized gliotoxin dithiol oxidase GliT (11). To evaluate a comparable function of HlmI as a *red*-holomycin oxidase, HlmI was expressed heterologously in *E.coli*

and purified as a yellow protein at a yield of 20 mg/L (Figure 4A and S2a). The bound cofactor was determined as FAD by LC/MS after heat denaturation of HlmI (Figure S2b and S2c) and was present in 0.2 molar equivalents to the 40 kDa protein. In vitro reconstitution by incubation with excess FAD resulted in an increase in FAD content to 0.76 equivalents. The apparent oligomeric state of HlmI was determined by gel filtration elution profile as dimeric.

To assay the activity of purified HlmI, holomycin, **1,** was reduced *in situ* in buffer solutions with one equivalent of TCEP to generate *red*-holomycin, **2**. The reduction process appeared to be complete as addition of excess TCEP did not further increase the UV absorbance at 340 nm, indicating that nearly all holomycin in solution had been reduced. Subsequent addition of HlmI led to rapid loss of the A_{340nm} peak as the dithiol substrate was oxidized to intramolecular disulfide in holomycin. A family of progression curves could be recorded to monitor reaction progress and enabled determination of the catalytic parameters of HlmI as a dithiol oxidoreductase for *red*-holomcyin (Figure 4B).

Concentration of **2** (from quantitative TCEP-mediated reduction of **1** *in situ*) was varied at a fixed concentration of HlmI (50 nM, effective concentration 10 nM based on 20% active enzyme by FAD content) to determine the steady-state kinetic parameters. A Michaelis-Menten curve was generated yielding a k_{cat} of 333±28 min^{-1} and a K_M of 4.6±1.9 μM for **2** (Figure 4C). Kinetic measurements using FAD recontituted HlmI with 0.76 equivalents of FAD generated similar results (Figure S3). In control experiments under the same incubation conditions without addition of enzyme, the non-enzymatic rate of reoxidation of **2** to **1** was monitored and a half life of 7 minutes was obtained for **2**, corresponding to a k_{uncat} of about 0.1 min^{-1} (Figure S4). The k_{cat}/k_{uncat} ratio for HlmI is 3330/1, suggesting a three order of magnitude rate enhancement in accelerating the disulfide formation. The half-life of reduced holomycin was not altered in the presence of EDTA, suggesting metal-mediated thiol oxidation was not responsible for the non-enzymatic formation of the intramolecular disulfide.

No electron receptors were added in the HlmI oxidation reaction suggesting that molecular oxygen is the terminal electron acceptor. Addition of nicotinamide cofactors (NAD^+ or $NADP^+$) did not increase the oxidation rate. Furthermore, HlmI failed to convert **2** to **1** under anaerobic conditions in the presence of NAD^+ or $NADP^+$, but readily catalyzed the disulfide formation once the reaction is opened to the atmosphere (Figure 4D). These results indicate that HlmI acts as a dithiol oxidase, similar to GliT. GliT has been proposed to use its active site disulfide as an initial redox port of entry for electrons from the dithiol substrate into FAD (11). The resulted $FADH_2$–Enzyme intermediate would be rapidly reoxidized by O_2, presumably through the canonical FAD-C_{4a}-OOH intermediate. Such a pathway for electron flow is also likely for HlmI, which contains a conserved CXXC motif (Figure S1). We propose that the FAD reductive half reaction is initiated by attack of the thiol group or the ene-thiol group of **2** on the active site disulfide in HlmI to yield a covalent disulfide adduct with the enzyme. Intramolecular attack of the second thiol upon proton abstraction by an active site base would lead to formation of the cyclic disulfide in **1** with generation of the reduced form of the enzyme (It is not known which thiol of **2** would initiate attack on the disulfide in the active site of HlmI; the enethiol, as a tautomer of a thiolaldehyde is likely to be less nucleophilic but nothing is known about the orientation of **2** in the enzyme active site) (Figure 5). FAD_{ox} then regenerates the active site disulfide in the enzyme to form $FADH_2$. Oxidation of $FADH_2$ by O_2 yields a transient FAD-C_{4a}-OOH on the way to release of hydrogen peroxide and regeneration of FAD_{ox}, presumably constituting the oxidative half reaction. The utilization of O_2 differentiates HlmI and GliT from DepH, which makes use of NAD^+ or $NADP^+$ as electron receptors (12).

GliT has reduced holomycin oxidase activity

Recombinant GliT was purified from *E. coli* (Dr. Carl Balibar thesis),[1] and contains 0.35 equivalents of bound FAD. We assayed GliT at 25 nM (effective concentration 8.75 nM with bound FAD) to determine whether it can oxidize **2** in addition to its normal substrate reduced gliotoxin (*red*-gliotoxin). This fungal dithiol oxidase can indeed oxidize **2** back to **1** (Figure 4C) with a K_M for **2** at 198±64 μM, 20–130 fold higher than HlmI. Interestingly, the measured k_{cat} was about 10 fold higher than HlmI, at 3166±742 min^{-1}. Similar K_M and k_{cat} values were obtained for GliT reconstituted with 0.8 equivalents of FAD (Figure S3). The k_{cat}/K_M catalytic efficiency ratios are 72 min^{-1} μM^{-1} for HlmI and 16 min^{-1} μM^{-1} for GliT for the oxidation of *red*-holomycin, respectively. Therefore HlmI is overall more efficient than GliT to make the cyclic disulfide in holomycin, but GliT is substantially promiscuous.

red-Holothin vs *red*-holomycin as HlmI substrates

During the initial characterization of the holomycin biosynthetic pathway, we demonstrated that an acetyltransferase HlmA encoded in the gene cluster catalyzes N-acetylation of holothin (deacetylated holomycin, see Figure 2B for structure) as a late step in the pathway (13). Acetylation of the exocyclic amino group of the dithiolopyrrolone was proposed to be involved in stabilizing the heterocyclic scaffold and/or be a self-protection strategy. We attempted to evaluate whether the reduced dithiol form of holothin could also be a substrate for HlmI. Holothin was generated by microwave-mediated deacetylation of holomycin and isolated in its oxidized form (13). Subsequent reduction of holothin by TCEP resulted in a blue shift in the UV spectrum consistent with the maximum absorbance around 340 nm observed in *red*-holomycin (Figure S5a). The dithiol group in *red*-holothin was much more prone to non-enzymatic oxidation to disulfide than *red*-holomycin. The half-life of *red*-holothin under aerobic conditions was very short, about 0.3 minutes (Figure S5b). HlmI qualitatively accelerated the reoxidation of red-holothin to holothin but the high non-enzymatic background rate precluded kinetic measurements. The significantly faster non-enzymatic oxidation of *red*-holothin compared to *red*-holomycin indicates that acetylation of the exocyclic amine of the aminopyrrolone ring confers a substantial electronic effect on the dithiol/disulfide redox properties. In both the N-acetylated *red*-holomycin and the free amine-containing *red*-holothin, the intramolecular dithiol groups are set up geometrically for facile closure to cyclic disulfide.

Phenotype of an HlmI deletion in *S. clavuligerus*

To assess the importance of HlmI in holomycin biosynthesis, we conducted targeted deletion of the *hlmI* gene in both the wild type *S. clavuligerus* and in the holomycin-overproducing strain (ΔORF15) in which ORF15 in the clavulanate biosynthetic pathway has been disrupted resulting in 10–100 fold overproduction of holomycin (21). The deletion of *hlmI* in both strains was verified by PCR analysis (Figure S6) and holomycin production was decreased by 10^2–10^3 folds in both strains (Figure 6A). Agar diffusion assays with pure holomycin demonstrated that *hlmI* deletions in wild type and ΔORF15 *S. clavuligerus* strains rendered both strains more susceptible toward holomycin (Figure 6B). This result suggests that HlmI protects the producer against the deleterious effects of holomycin at a high concentration. Similarly, it was reported that deletion of *gliT* in gliotoxin pathway abolished gliotoxin production and led to increased sensitivity of the producing strain toward gliotoxin (11, 22). Similar to gliotoxin, holomycin may also exist in the inactive disulfide form and become reduced in the cellular environment yielding the active form of the antibiotic. The dithiol oxidase HlmI may act as a protective catalyst against holomycin in the producing *S. clavuligerus* strain.

[1]Purified GliT was generously provided by Dr. Carl Balibar, a previous graduate student in the Walsh group.

Dithiol-disulfide reactivity in holomycin

It is not clear whether holomycin plays physiological roles other than self-defense for its producing strain. The exact mechanism of action against target microbes has yet to be determined. Although holomycin was shown to block RNA synthesis in whole bacteria and RNA polymerases have been suggested as holomycin targets, *E. coli* RNA polymerases are not susceptible toward holomycin in *in vitro* assays (7). The disulfide embedded in a conjugated bicyclic framework is likely to engage in dithiol-disulfide redox chemistry with holomycin targets. We have conducted an initial examination of holomycin reactivity with the most abundant cellular thiol, glutathione, as a prototypic marker of redox behavior. We first incubated the disulfide-containing holomycin with the reduced form of glutathione (GSH) and monitored for reduction of holomycin by gain of UV absorbance at 340 nm. No changes were detected over a wide range of GSH concentrations and molar excess over **1**. When we assayed in the opposite direction, for the ability of **2** to reduce oxidized glutathione (GS-SG), a rapid decrease in UV absorbance at 340 nm was observed, corresponding to the oxidation of **2** by GS-SG. The rate of oxidation of **2** as a function of oxidized GS-SG is shown in Figure S7.

Subsequent studies will be necessary to determine redox equilibria and ultimately reduction potentials of holomycin under conditions where competing oxidation by molecular O_2 is suppressed. It is clear that *red*-holomycin is kinetically and thermodynamically competent to reduce the intermolecular disulfide in oxidized glutathione. Thus, the reduced form of holomycin and presumably holothin (perhaps even more so) may be strong thiol reductants in both microbial producers and target cells. The combination of oxidation by HlmI and acetylation by HlmA may ensure accumulation of the natural product in the oxidized and acetylated state with low adventitious redox reactivity. Future studies will involve the examination of the formation of any mixed disulfides between holomycin and intracellular proteins as part of the antibacterial effect of holomycin and related dithiolopyrrolone scaffolds.

An alternative mode of reactivity is also possible involving conjugated addition of cellular nucleophiles to the dienone chromophore for holomycin. Amine nucleophiles such as N-acetylcysteamine to a certain degree perturbed the UV spectrum of holomycin by changing its λ_{max} at 385 nm in buffered solutions at pH 9 (Figure S8), although no adduct formation has been observed by LC-MS suggesting that the conjugated Michael-addition of amines with holomycin may be transient.

Phylogeny analysis of HlmI

Alignment of HlmI with a number of bacterial and fungal proteins that are likely to catalyze dithiol-disulfide redox chemistry revealed four distinctive phylogeny groups: the thioredoxin oxidoreductase (TrxB) group, and three small molecule oxidoreductase groups (Figure 7 and S8). The TrxB group catalyzes the reduction of disulfides in thioredoxins, which are small proteins involved in a wide range of cellular processes such as redox-sensitive signal transduction, stress response, and detoxification (23). This group includes both bacterial and fungal thioredoxin oxidoreductases. Interestingly among the small molecule oxidoreductases, HlmI, GliT and DepH belong to three different groups. The GliT group consists of fungal proteins from gene clusters for biosyntheses of molecules closely related to gliotoxin, and is likely differentiated from the HlmI and DepH groups because of its fungal origin. The DepH group contains a number of bacterial putative oxidoreductases including TdpH encoded in a FK228 homologous gene cluster from *Burkholderia thailandensis* E264. The products of this gene cluster have recently been identified as burkholdac A and B, which are new HDAC inhibitors containing an intramolecular disulfide (24). Many hypothetical proteins in the HlmI group are predicted dithiol-disulfide

oxidoreductases, and they may be involved in similar cellular processes such as small molecule biosynthesis or detoxification. Further interrogation of the genome context of these hypothetical proteins may lead to the discovery of novel natural product biosynthetic gene clusters.

Summary

HlmI joins GliT as a member of FAD-dependent dithiol oxidases, using O_2 as cosubstrate to accelerate the formation of intramolecular disulfide bridges in the late steps of small molecule biosynthesis. These two enzymes differ from the FK228 dithiol oxidase DepH, which utilizes $NADP^+$ as the electron acceptor. Both HlmI and GliT were shown to play a role in protecting the producer organisms from the action of their own natural products. Similar to gliotoxin and FK228, the reduced dithiol form of holomycin may be the active form of the antibiotic, and the redox properties of the thiol/enethiol pair in reduced holomycin remain to be examined. HlmI and related proteins constitute a new phylogenetic group of oxidoreductases that catalyze disulfide formation in small molecules and are different from the GliT and DepH dithiol oxidase groups. These small molecule dithiol oxidases are phylogenetically separated from the peptide oxidoreductases, suggesting they have evolved for specific and efficient catalysis of small molecule substrates.

Supplementary Material

Refer to Web version on PubMed Central for supplementary material.

Abbreviations

***red*-holomycin**	reduced holomycin
***red*-holothin**	reduced holothin
***red*gliotoxin**	reduced gliotoxin
***red*-FK228**	reduced FK228
HDAC	histone deacetylase
FAD	flavin adenine dinucleotide
NRPS	nonribosomal peptide synthetase
IPTG	isopropyl-β-D-thiogalactopyranoside
TCEP	tris(2-carboxyethyl)phosphine
GSH	glutathione
GS-SG	oxidized glutathione
NAD^+	nicotinamide adenine dinucleotide
$NADP^+$	nicotinamide adenine dinucleotide phosphate
SDS-PAGE	sodium dodecyl sulfate-polyacrylamide gel electrophoresis
HPLC	high-performance liquid chromatography
LC-MS	liquid chromatography-mass spectrometry

Acknowledgments

We thank Dr. Carl Balibar for the generous gift of purified GliT, Dr. Kapil Tahlan for providing *S. clavuligerus* ORF15::*apr* mutant, Dr. Emily Balskus and Dr. Rebecca Case for assistance in constructing the phylogeny tree, and Dr. Albert Bowers for suggestions regarding the manuscript.

This research is financially supported by NIH Grant GM49338 (CTW).

References

1. Celmer WD, Solomons IA. The structures of thiolutin and aureothricin, antibiotics containing a unique pyrrolinonodithiole nucleus. J. Am. Chem. Soc. 1955; 77:2861–2865.
2. Kenig M, Reading C. Holomycin and an antibiotic (MM 19290) related to tunicamycin, metabolites of *Streptomyces clavuligerus*. J. Antibiot. (Tokyo). 1979; 32:549–554. [PubMed: 468729]
3. McInerney BV, Gregson RP, Lacey MJ, Akhurst RJ, Lyons GR, Rhodes SH, Smith DR, Engelhardt LM, White AH. Biologically active metabolites from Xenorhabdus spp., Part 1. Dithiolopyrrolone derivatives with antibiotic activity. J. Nat. Prod. 1991; 54:774–784. [PubMed: 1955880]
4. Shiozawa H, Kagasaki T, Kinoshita T, Haruyama H, Domon H, Utsui Y, Kodama K, Takahashi S. Thiomarinol, a new hybrid antimicrobial antibiotic produced by a marine bacterium. Fermentation, isolation, structure, and antimicrobial activity. J. Antibiot. (Tokyo). 1993; 46:1834–1842. [PubMed: 8294241]
5. Jimenez A, Tipper DJ, Davies J. Mode of action of thiolutin, an inhibitor of macromolecular synthesis in *Saccharomyces cerevisiae*. Antimicrob. Agents Chemother. 1973; 3:729–738. [PubMed: 4597739]
6. Tipper DJ. Inhibition of yeast ribonucleic acid polymerases by thiolutin. J. Bacteriol. 1973; 116:245–256. [PubMed: 4583213]
7. Oliva B, O'Neill A, Wilson JM, O'Hanlon PJ, Chopra I. Antimicrobial properties and mode of action of the pyrrothine holomycin. Antimicrob. Agents Chemother. 2001; 45:532–539. [PubMed: 11158751]
8. Ireland DC, Clark RJ, Daly NL, Craik DJ. Isolation, sequencing, and structure-activity relationships of cyclotides. J. Nat. Prod. 2010; 73:1610–1622. [PubMed: 20718473]
9. Newkirk TL, Bowers AA, Williams RM. Discovery, biological activity, synthesis and potential therapeutic utility of naturally occurring histone deacetylase inhibitors. Nat. Prod. Rep. 2009; 26:1293–1320. [PubMed: 19779641]
10. Gardiner DM, Waring P, Howlett BJ. The epipolythiodioxopiperazine (ETP) class of fungal toxins: distribution, mode of action, functions and biosynthesis. Microbiology. 2005; 151:1021–1032. [PubMed: 15817772]
11. Scharf DH, Remme N, Heinekamp T, Hortschansky P, Brakhage AA, Hertweck C. Transannular disulfide formation in gliotoxin biosynthesis and its role in self-resistance of the human pathogen Aspergillus fumigatus. J. Am. Chem. Soc. 2010; 132:10136–10141. [PubMed: 20593880]
12. Wang C, Wesener SR, Zhang H, Cheng YQ. An FAD-dependent pyridine nucleotide-disulfide oxidoreductase is involved in disulfide bond formation in FK228 anticancer depsipeptide. Chem. Biol. 2009; 16:585–593. [PubMed: 19549597]
13. Li B, Walsh CT. Identification of the gene cluster for the dithiolopyrrolone antibiotic holomycin in Streptomyces clavuligerus. Proc. Natl. Acad. Sci. U. S. A. 2010; 107:19731–19735. [PubMed: 21041678]
14. Huang S, Zhao Y, Qin Z, Wang X, Onega M, Chen L, He J, Yu Y, Deng H. Identification and heterologous expression of the biosynthetic gene cluster for holomycin produced by *Streptomyces clavuligerus*. Process Biochem. 2011
15. Cramer RA Jr, Gamcsik MP, Brooking RM, Najvar LK, Kirkpatrick WR, Patterson TF, Balibar CJ, Graybill JR, Perfect JR, Abraham SN, Steinbach WJ. Disruption of a nonribosomal peptide synthetase in Aspergillus fumigatus eliminates gliotoxin production. Eukaryot Cell. 2006; 5:972–980. [PubMed: 16757745]

16. Okamura K, Soga K, Shimauchi Y, Ishikura T, Lein J. Holomycin and N-propionylholothin, antibiotics produced by a cephamycin C producer. J. Antibiot. (Tokyo). 1977; 30:334–336. [PubMed: 863793]

17. Gust B, Challis GL, Fowler K, Kieser T, Chater KF. PCR-targeted Streptomyces gene replacement identifies a protein domain needed for biosynthesis of the sesquiterpene soil odor geosmin. Proc. Natl. Acad. Sci. U. S. A. 2003; 100:1541–1546. [PubMed: 12563033]

18. Kieser, T.; Bibb, MJ.; Buttner, MJ.; Chater, KF.; Hopwood, DA. Practical Streptomyces Genetics. Norwich, UK: John Innes Foundation; 2000.

19. Romero J, Liras P, Martin JF. Utilization of ornithine and arginine as specific precursors of clavulanic acid. Appl. Environ. Microbiol. 1986; 52:892–897. [PubMed: 2877616]

20. Stamatakis A. RAxML-VI-HPC: maximum likelihood-based phylogenetic analyses with thousands of taxa and mixed models. Bioinformatics. 2006; 22:2688–2690. [PubMed: 16928733]

21. de la Fuente A, Lorenzana LM, Martin JF, Liras P. Mutants of *Streptomyces clavuligerus* with disruptions in different genes for clavulanic acid biosynthesis produce large amounts of holomycin: possible cross-regulation of two unrelated secondary metabolic pathways. J. Bacteriol. 2002; 184:6559–6565. [PubMed: 12426344]

22. Schrettl M, Carberry S, Kavanagh K, Haas H, Jones GW, O'Brien J, Nolan A, Stephens J, Fenelon O, Doyle S. Self-protection against gliotoxin--a component of the gliotoxin biosynthetic cluster, GliT, completely protects *Aspergillus fumigatus* against exogenous gliotoxin. PLoS Pathog. 2010; 6 e1000952.

23. Meyer Y, Buchanan BB, Vignols F, Reichheld JP. Thioredoxins and glutaredoxins: unifying elements in redox biology. Annu. Rev. Genet. 2009; 43:335–367. [PubMed: 19691428]

24. Biggins JB, Gleber CD, Brady SF. Acyldepsipeptide HDAC Inhibitor Production Induced in *Burkholderia thailandensis*. Org. Lett. 2011

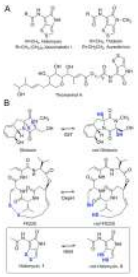

Figure 1.
(A) Structures of holomycin and related dithiolopyrrolone antibiotics. (B) Conversion of the reduced form of holomycin, gliotoxin and FK228 into the disulfide form by thioredoxin oxidoreductase-like enzymes.

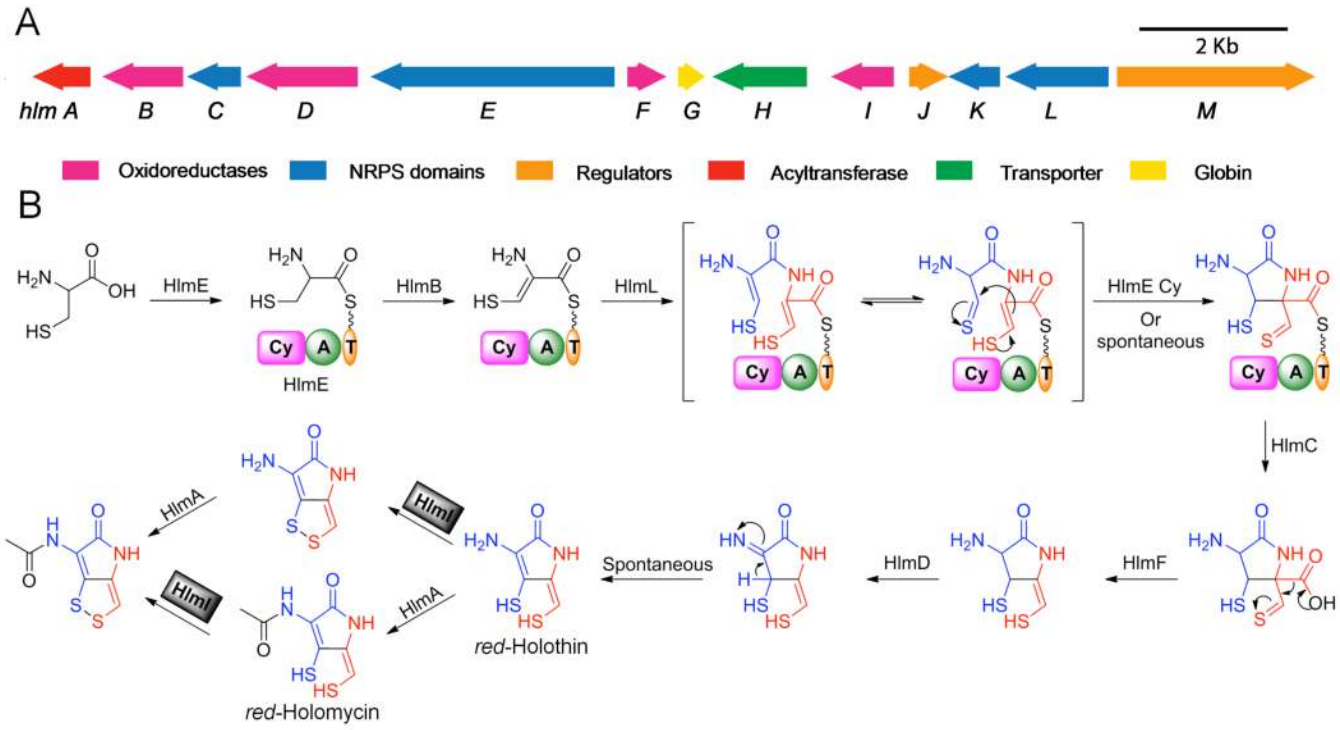

Figure 2.

(A) Holomycin (*hlm*) gene cluster with genes colored by function. *hlmA*, acyltranferase; *hlmB*, acyl-CoA dehydrogease; *hlmC*, thioesterase; *hlmD*, glucose-methanol-choline oxidoreductase; *hlmE*, NRPS (Cyclization-Adenylation-Thiolation, Cy-A-T); *hlmF*, lantibiotic decarboxylase; *hlmG*, globin; *hlmH*, major facilitator family transporter; *hlmI*, thioredoxin-disulfide oxidoreductase; *hlmJ*, *hlmM*, transcriptional regulators; *hlmK*, inactive thioesterase domain; *hlmL*, condensation domain. (B) Proposed holomycin biosynthetic pathway. HlmI, the focus of this study, is shown in a highlighted box, and is proposed to be involved in the late stages of holomycin biosynthesis.

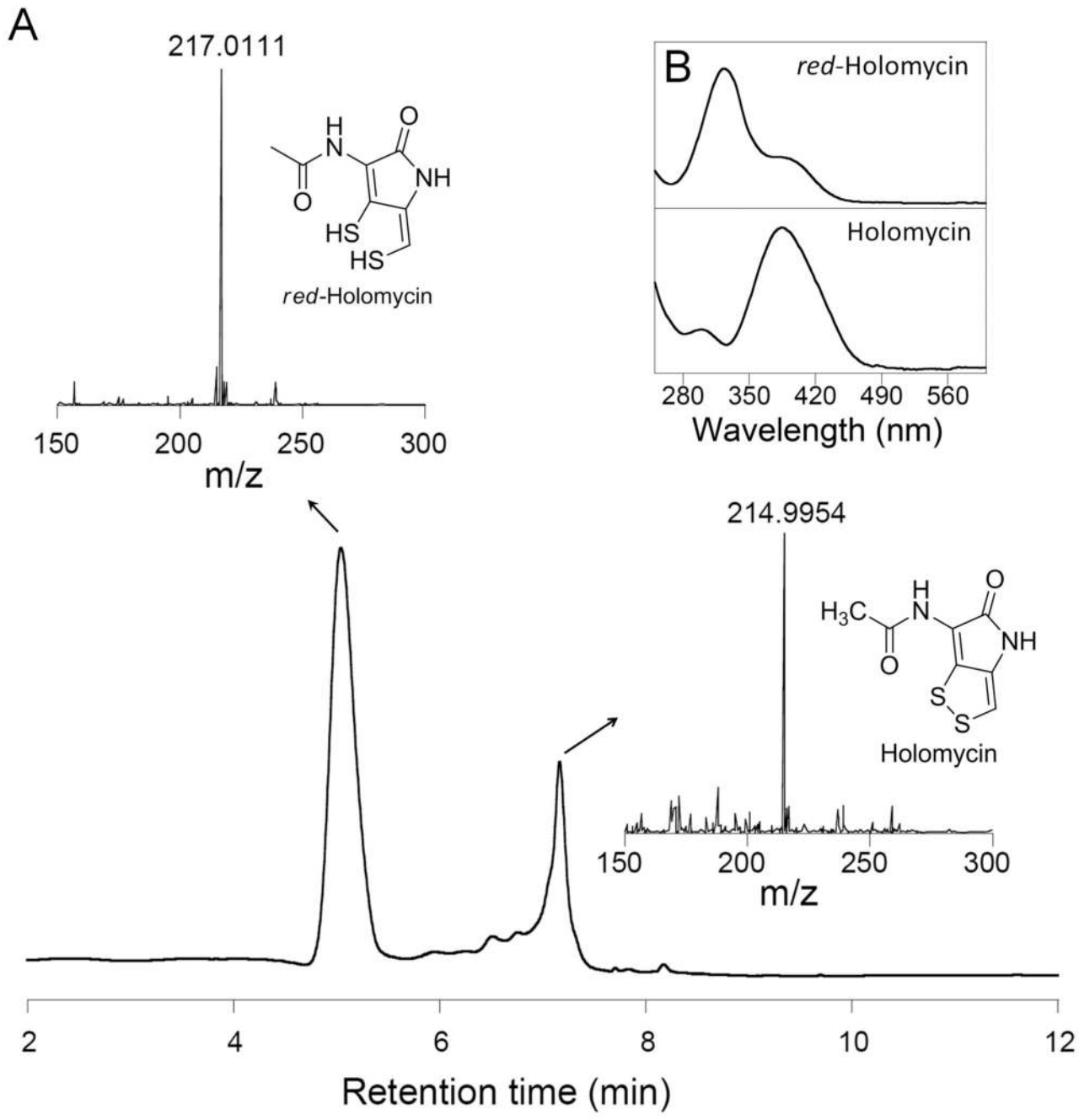

Figure 3.

(A) LC-MS analysis of holomycin treated with 2 equivalent of TCEP. UV trace at 390 nm is shown with a clear separation of *red*-holomycin (5.0 min) and holomycin (7.2 min). The presence of holomycin in the UV trace is due to the reoxidation of *red*-holomycin by O_2 during the sample injection and column separation. (B) UV spectra of *red*-holomycin and holomycin.

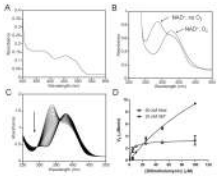

Figure 4.

(A) UV-visible absorbance spectrum of HlmI containing 20% of FAD. (B) Time course of oxidation of 100 μM *red*-holomycin by 50 nM HlmI in 10 min (UV spectra scan was taken every 0.4 min). Arrow indicates the direction of UV spectra progression. (C) Michaelis-Menten kinetics curve of HlmI (20% FAD) and GliT (35% FAD) with varying concentrations of *red*-holomycin substrate. Standard deviation is shown as error bars. (D) Anaerobic assay of 50 μM of dithiolholomycin and 50 nM HlmI in the presence of 1 mM NAD^+ (NAD^+, no O_2). HlmI was unable to convert **2** to **1** without oxygen. When the assay was opened to the atmosphere (NAD^+, O_2), facile oxidation of **2** to **1** by HlmI was observed. Substitution of NAD^+ with $NADP^+$ yielded the very similar results and therefore is not shown in the graph.

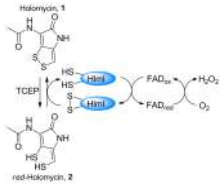

Figure 5.
Proposed mechanism of catalysis by HlmI to convert *red*-holomycin to holomycin.

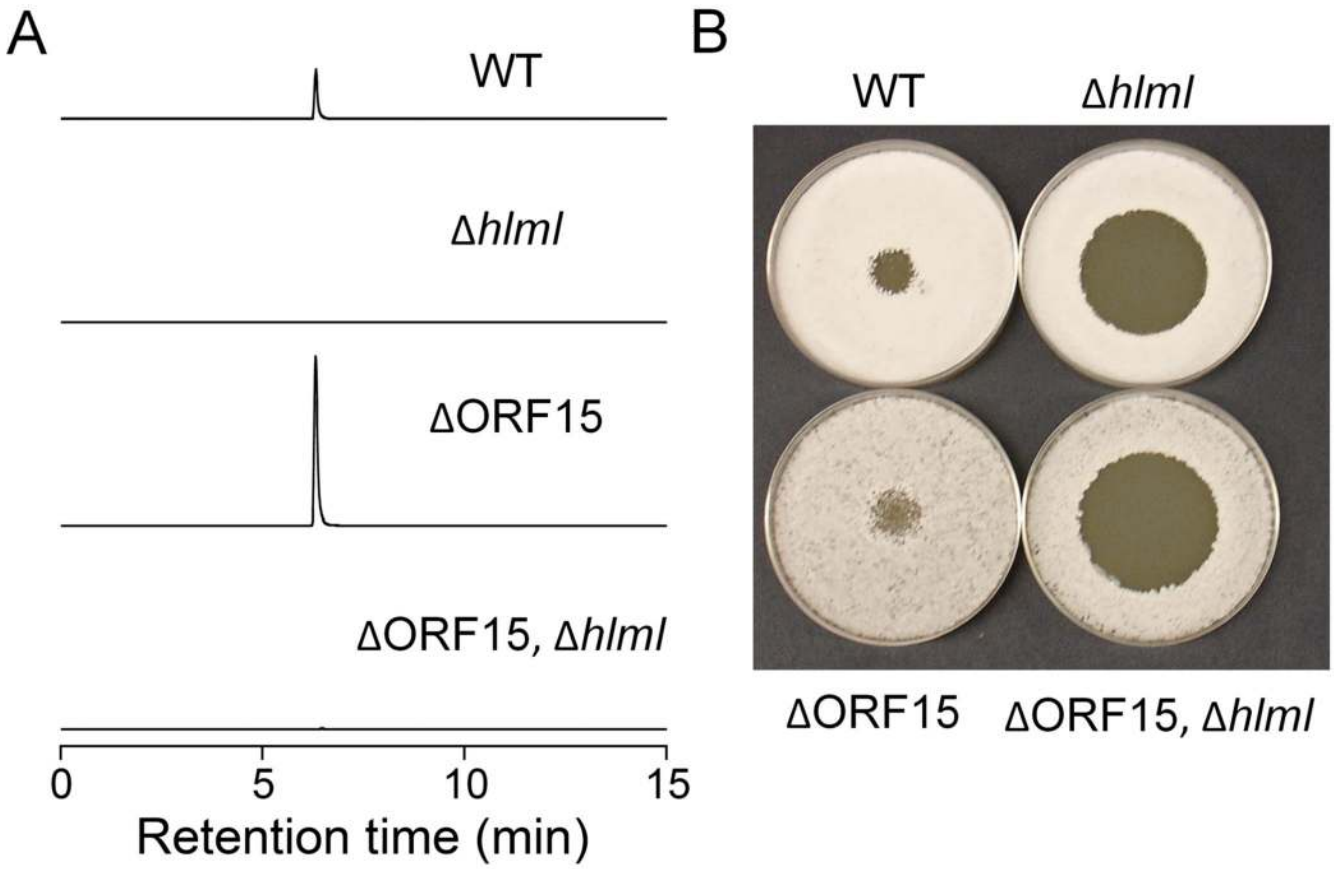

Figure 6.

Phenotypes of *hlmI* deletion mutants in wild type *S. clavuligerus* and holomycin-overproducing strain (ΔORF15). (A) Holomycin production by four *S. clavuligerus* strains as determined by LC-MS. Mass extraction results are shown for holomycin ($[M + H]^+$, 214.9943) allowing for 20 ppm error. The level of holomycin produced by Δ*hlmI* and Δ*hlmI*/ΔORF15 strains was decreased by 10^2-10^3 folds in comparison to that of wild type and the ΔORF15 mutant and therefore did not show in the trace when the mass intensity is normalized to the level of holomycin production in ΔORF15. (B) Sensitivity of four *S. clavuligerus* strains toward holomycin determined in an agar diffusion inhibition assay. A sample of 5 μL of 7 mg/mL holomycin was added onto a lawn of freshly plated bacteria and incubated at 30 °C for 5 days.

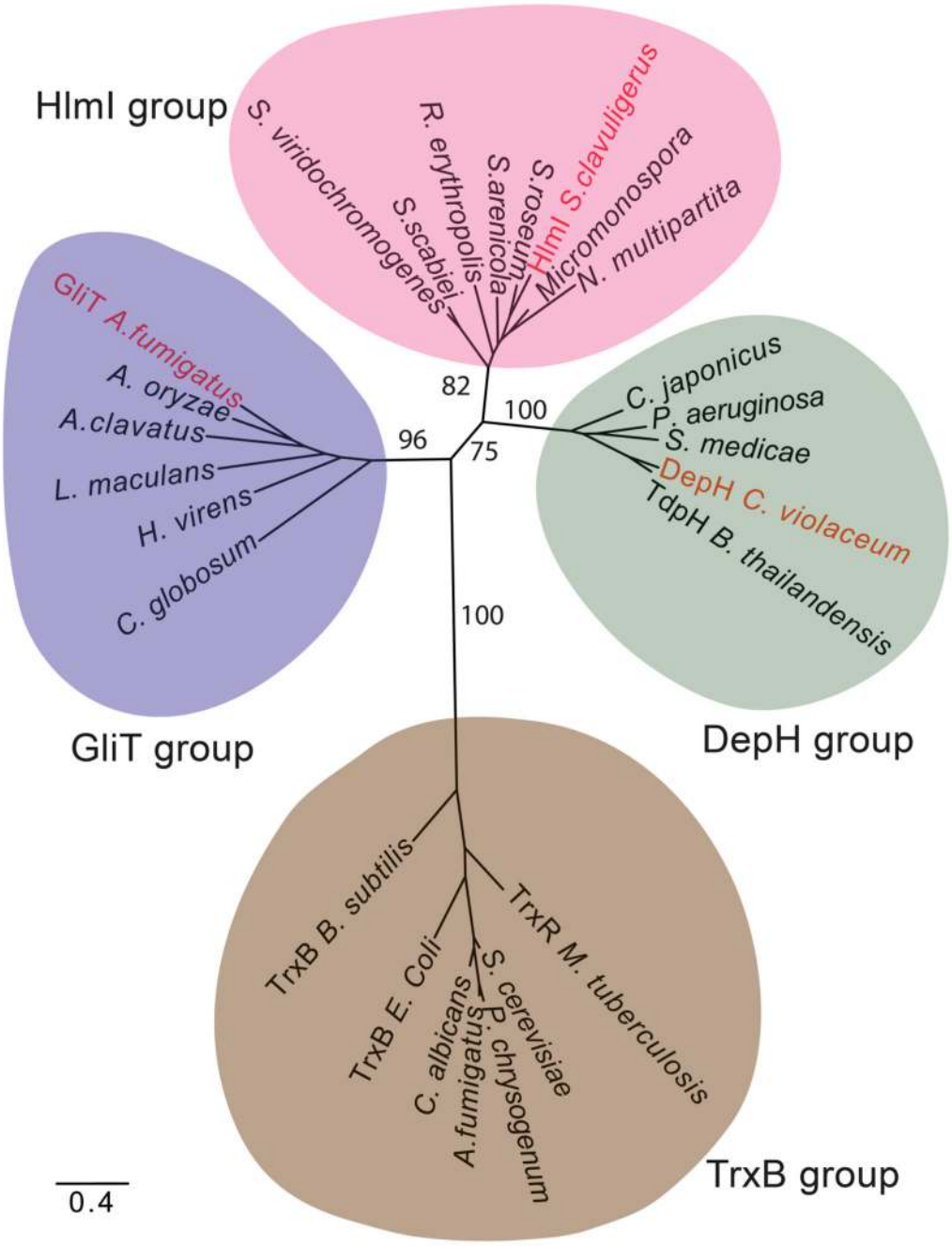

Figure 7.

Phylogenetic analysis of HlmI and HlmI homologs (HlmI group), DepH and homologs (DepH group), GliT and holomologs from other ETP fungal clusters (GliT group), thioredoxin reductase-like proteins from bacteria and fungi (TrxB group). This dendrogram is generated by RAxML and bootstrap support values and the distance scale are displayed.